alkylpentafluorocyclotriphosphazenes were examined in order to clarify differences between σ and π donor substituent effects. The fact that the alkylphosphazenes undergo the phenylation reaction unambiguously demonstrates that π donation from the exocyclic function is not a necessary prerequisite for this reaction to be effective. The significantly higher yield in the reaction of *tert*-butyl vs. the *n*-butyl phosphazene suggests the operation of a mechanism wherein the phoshorus atom undergoing substitution goes to a lower coordinate intermediate (or transition state). This process would be most favorable for the *tert*-butyl derivative, where the maximum relief of steric strain can be obtained. A reasonable model for the Friedel–Crafts phenylation reaction of substituted phosphazenes is one in which the substituted phosphorus atom goes through a three-coordinate phosphorus(V) intermediate which is stabilized by the σ-electron-releasing nature of the substituent. It is possible that, in the phenyl and dialkylamino systems, the σ-electron-releasing effect may be supplemented by a π effect, but conclusive evidence of this has yet to be presented. The reluctance of the ethoxypentafluorocyclotriphosphazene to enter into the Friedel–Crafts reaction is consistent with these proposals since the high electronegativity of the oxygen atom makes it a poor electron-releasing substituent and the small size does not allow for significant relief of steric strain on going to a lower coordinate transition state intermediate.

Acknowledgment. Phosphazene chemistry at the University of Vermont is supported in part by the Office of Naval Research. We wish to thank Firestone Corp. for a generous gift of hexachlorocyclotriphosphazene and Mr. Weglarz for checking certain synthetic results. The X-ray work at Arkansas was supported by the State of Arkansas and the National Science Foundation (EPSCOR Grant ISP801147).

Registry No. **1**, 95979-67-2; **2**, 95979-68-3; **3**, 95979-69-4; $N_3P_3F_5N(CH_3)_2$, 23208-17-5; $N_3P_3F_5CH_2(CH_2)_2CH_3$, 650-08-8; $N_3P_3F_5C(CH_3)_3$, 81095-56-9; $N_3P_3F_5OCH_2CH_3$, 33027-66-6; C_6H_6, 71-43-2.

Supplementary Material Available: Table S1 showing major mass spectral fragments and their intensities, Table S2 showing structure factor amplitudes for $N_3P_3F_4(C_6H_5)(C_4H_9)$, and Table S3 showing anisotropic thermal parameters for $N_3P_3F_4(C_6H_5)(C_4H_9)$ (13 pages). Ordering information is given on any current masthead page.

Contribution from Baker Laboratory of Chemistry,
Cornell University, Ithaca, New York 14853

Structure and Superconductivity in Lithium-Intercalated Niobium Dichalcogenides

C. S. McEWEN, D. J. St. JULIEN,* P. P. EDWARDS,† and M. J. SIENKO‡

Received August 11, 1983

The series Li_xNbS_2 ($0 \le x \le 0.50$) and Li_xNbSe_2 ($0 \le x \le 0.67$) have been prepared by high-temperature reaction of Li_2S, Nb, and S or Li_2Se, Nb, and Se. Structures have been determined by analysis of X-ray powder patterns with polytypism observed in the sulfide series. Evidence of staging and Li ordering is reported, and crystal parameters are proposed for a second-staged sample, $Li_{0.2}NbSe_2$. In the series Li_xNbSe_2, T_c exhibits a monotonic decrease with increasing lithium content, falling to less than 2 K by $x = 0.25$. In contrast, in the Li_xNbS_2 series, T_c exhibits a more complicated pattern with T_c plummeting to below 2 K by $x = 0.05$, only to rebound to 3.7 K at $x = 0.33$ and then fall to below 2 K by $x = 0.4$.

Introduction

Among the many unusual properties of the layered transition-metal dichalcogenides, one of the most interesting is the occurrence of moderately high superconducting critical temperatures (6.4 K for NbS_2 and 7.8 K for $NbSe_2$). The superconducting critical temperature, T_c, has been shown to be dependent upon, among other things, the rigidity of the crystal lattice and the density of electronic states, $N(E_F)$, at the Fermi level. If we add electrons to a superconducting material, we expect to see, depending on the shape of the conduction band, either an increase or a decrease in T_c. In many layered materials the Fermi level may be adjusted by the intercalation of alkali metals. Intercalation results in charge transfer from the guest alkali-metal atom to the host dichalcogenide. The intercalate may also alter the structure of the host and may itself form an ordered array within the host. Alkali-metal intercalation of superconducting layered transition-metal dichalcogenides, therefore, promises to yield a host of possible structural and electronic effects, and T_c provides a sensitive tool by which to measure them.

In the present work we have prepared at high temperature two series of alkali-metal intercalated transition-metal dichalcogenides, Li_xNbSe_2 and Li_xNbS_2 ($0 \le x < 1$). We have examined the basic structural parameters, *a* and *c*, and have followed the change in T_c brought on by intercalation.

Experimental Section

For Li_xNbS_2, the starting materials were niobium foil ("Marz" grade, from Materials Research Corp.), Li_2S (99.9%, Cerac, Inc.), and sulfur (99.9999%, Atomergic Chemicals Corp.). X-ray analysis of the commercial Li_2S yielded no evidence of impurities. Amounts of Nb, Li_2S, and S, calculated to give a total sulfur overpressure of 8 atm at the anneal temperature of 750 °C, were added to degassed heavy-walled fused silica tubes in a helium-atmosphere Dri-Lab. After evacuation to 10^{-6} torr, the tubes were sealed and the samples were gradually raised to 950 °C over a period of 8 days. After 1 week at 950 °C, the samples were cooled (at 5 °C/h) to 750 °C, annealed at 750 °C for 4 days, and then quenched into cold water. (Quenching separates the product from the excess sulfur and prevents formation of NbS_3.) All of the samples were then thoroughly ground in the Dri-Lab, resealed with an appropriate amount of sulfur, heated to 950 °C for 1 week, annealed at 750 °C, and quenched.

The products were silvery polycrystalline materials or black finely divided powders. The crystallinity of the samples increased with lithium concentration. It was not possible to make Li_xNbS_2 ($x > 0.50$) samples in this way because of tube attack by the lithium.

Nominally stoichiometric $LiNbS_2$ was obtained by reaction of niobium disulfide with excess *n*-butyllithium in hexane. The mixture was allowed to sit for 10 days (in a nitrogen-atmosphere drybox) and then filtered and rinsed with dry hexane. The product was dried under vacuum and stored, together with all the other samples, in the Dri-Lab. The Li_xNbS_2 samples were found to be only moderately moisture sensitive and could be handled in air for brief periods.

Samples of nominal composition Li_xNbSe_2 ($0 \le x \le 0.67$) were prepared by direct, high-temperature reaction of "Marz" grade niobium foil, Li_2Se (99.9%, Cerac, Inc.), and selenium (99.9999%, Atomergic Chemical Corp.). Samples were prereacted at 400 °C for 1 day and then heated gradually from 600 to 800 °C at 5 °C/h. They were were kept at 800 °C for 1 week, slow-cooled to room temperature, ground in a Dri-Lab, resealed, and heated up to 800 °C again. After a final treatment of 5 days, they were slow-cooled to room temperature. All of the materials were silver-green microcrystalline powders. It was not possible to make Li_xNbSe_2 with $x > 0.67$ this way because of tube attack by lithium. As before, nominally stoichiometric $LiNbSe_2$ was prepared by reaction of $NbSe_2$ with *n*-butyllithium. All of the Li_xNbSe_2 products were moisture sensitive.

† Permanent address: University Chemical Laboratory, Lensfield Road, Cambridge CB2 1EW, U.K.
‡ Deceased.

0020-1669/85/1324-1656$01.50/0 © 1985 American Chemical Society

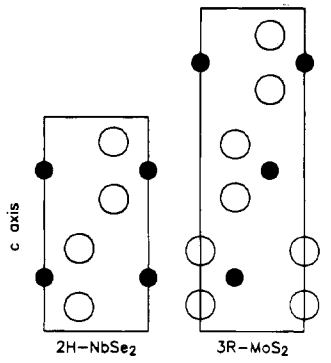

Figure 1. 110 projections of the 2H-$NbSe_2$ and 3R-MoS_2 structures. ● and ○ represent metal and chalcogen atoms, respectively.

Table I. Li_xNbSe_2 Lattice Parameters and Superconductivity Data

x in Li_xNbSe_2	a, Å[a,b]	c, Å[a,c]	T_c, K	ΔT_c, K
0.00	3.4444	2× 6.271	7.44	0.12
0.01	3.4444	2× 6.281	7.48	0.14
0.03	3.4467	2× 6.303	7.02	0.21
0.05	3.4466	2× 6.325	6.77	0.57
0.10	3.4493	2× 6.377	5.83	0.27
0.15	3.4518	2× 6.425	4.68	0.64
0.20	3.4541	2× 6.474	2.54	0.30
			2.41	0.25
0.25	3.4567	2× 6.524	1.87	0.21
0.33	3.4616	2× 6.615	<1.78	
0.50	3.4667	2× 6.689	<1.75	
0.67	3.4697	2× 6.720	<1.75	
1.00	3.500 (1)	2× 6.776 (4)	<1.75	

[a] Parentheses denote the estimated error for sample with larger errors. [b] ±0.004 Å. [c] ±0.001 Å.

Composition Analysis. The samples intercalated by the *n*-butyllithium method were analyzed for lithium content by flame emission spectrometry. The compositions determined were $Li_{0.89\pm0.02}NbS_2$ and $Li_{0.84\pm0.01}NbSe_2$, assuming transition-metal-to-chalcogen ratio of 1:2. We also analyzed one of the high-temperature samples ($Li_{0.35}NbS_2$) and found slightly less lithium than the nominal composition suggests ($Li_{0.31\pm0.01}NbS_2$). In this paper nominal compositions will be quoted although actual lithium content may be slightly less.

Powder X-ray diffraction patterns were obtained in sealed capillaries with a 114.6 mm diameter Debye-Scherrer camera with nickel-filtered copper Kα radiation. The data were analyzed as described previously.[1] For intensity calculations, powder patterns from a Guinier-Simon camera with a bent-crystal monochrometer were used. Intensities were read with a computer-interfaced Joyce Loebl microdensitometer.

Superconducting transition temperatures were determined by an ac mutual inductance technique using equipment previously described.[1] T_c was taken as the midpoint of the susceptibility transition and ΔT_c, the width of the transition, as the temperature difference between the points where the transition was 10% and 90% complete.

Some of the samples were observed to have two T_c's, which often overlapped. In such cases, T_c and ΔT_c were determined by visually estimating how two separate transitions could give riise to the observed result. These values are less precise.

Results and Discussion

Li_xNbSe_2. The structure of Li_xNbSe_2 was found to be that of the end member 2H-$NbSe_2$ for the entire series from $x = 0$ to $x = 1$. This structure is shown in Figure 1. Lattice-parameter data are listed in Table I and plotted in Figure 2. For the sake of comparison, the results of Dahn and Haering[2] for room-temperature electrochemical intercalation are also shown. As seen in Figure 2, the a parameter increases linearly with x between $x = 0$ and $x = 0.33$. The samples with $x > 0.33$ deviate from linearity due to lithium lost by reaction with the sample tube. The $x = 1$ sample was prepared at room temperature by reaction with

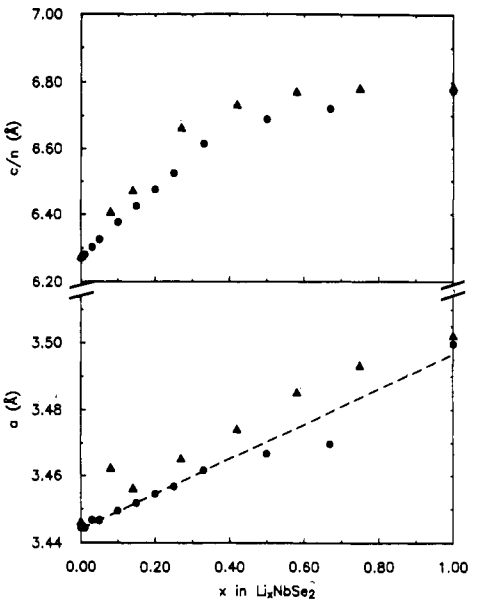

Figure 2. Lattice parameters vs. nominal composition in Li_xNbSe_2. ● and ▲ represent our results and those of Dahn and Haering,[2] respectively; the dashed line is a fit to our data at low x.

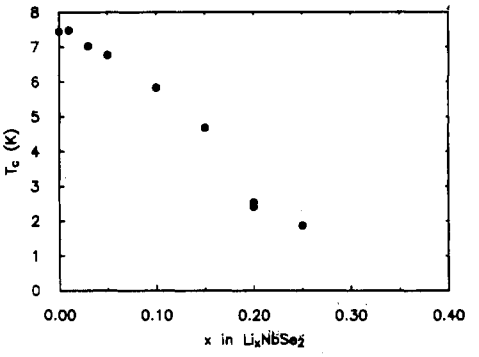

Figure 3. Superconducting critical temperature vs. nominal composition in Li_xNbSe_2.

n-butyllithium, and its a parameter (3.500 Å) compares favorably with other reported values of 3.496,[3] 3.502,[4] and 3.502 Å.[2] As seen in Figure 2, the a parameter of our high-temperature synthesis extrapolates to a value of 3.496 Å for $x = 1$, which agrees well with the low-temperature results.

The c parameter (Figure 2) rises very quickly and then appears to change very little after $x = 0.33$. This agrees qualitatively with the results of Dahn and Haering[2] and has been observed by Thompson and others in TaS_2 and TiS_2.[5] The c axis expands linearly below $x = 0.33$ with a slope of about 1 Å/Li/layer. This expansion is almost 20 times that of the a axis and is in agreement with Thompson's hypothesis that the rapid increase in c is due to increased electrostatic repulsions between the layers. Our measured value of c for $x = 1$ (13.552 Å) again compares favorably with reported values of 13.544,[3] 13.60,[4] and 13.57 Å.[2]

The superconducting critical temperature (T_c) for the system Li_xNbSe_2 was observed to decrease monotonically from 7.44 K at $x = 0$ to less than 2 K at $x = 0.25$ (Table I and Figure 3). This result may be explained in terms of the band structures of Matthiess and others.[6] If a rigid band model is assumed, then the addition of lithium between the layers leads to the addition of electrons to the half-filled d_{z^2} band. This moves the density of states away from its maximum, and the resulting decrease in $N(E_F)$ reduces the T_c. These results can be compared with the

(1) Fisher, W. G.; Sienko, M. J. *Inorg. Chem.* **1980**, *19*, 39.
(2) Dahn, D. C.; Haering, R. R. *Solid State Commun.* **1982**, *44*, 29.
(3) Whittingham, M. S.; Gamble, R. R. Jr. *Mater. Res. Bull.* **1975**, *10*, 363.
(4) Murphy, D. W.; Di Salvo, F. J.; Hull, G. W.; Waszczak, J. V. *Inorg. Chem.* **1976**, *15*, 17.
(5) Thompson, A. H.; Symon, C. R. *Solid State Ionics* **1981**, *3/4*, 175.
(6) Matthiess, L. F. *Phys. Rev. B: Solid State* **1973**, *8*, 3719.

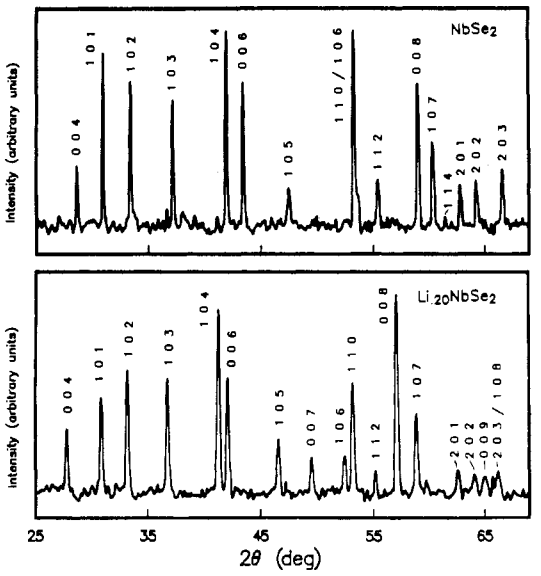

Figure 4. Debye-Scherrer powder patterns for $NbSe_2$ and $Li_{0.20}NbSe_2$. The $Li_{0.20}NbSe_2$ pattern shows lines with Miller indices 007 and 009.

work of Revolinsky, Spiering, and Beernsten[7] on $Nb_{1+x}Se_2$, where a similar decrease was observed.

Samples in the series Li_xNbSe_2 exhibited X-ray powder patterns as anticipated for the expanded end member $NbSe_2$. Lines with Miller indices $h - k = 3n$ were systematically absent unless $l = 2n$, as expected for space group $P6_3/mmc$. The sample $Li_{0.20}NbSe_2$, however, exhibited a number of forbidden lines. Figure 4 shows portions of Debye–Scherrer X-ray powder patterns for $NbSe_2$ and $Li_{0.20}NbSe_2$. Integrated intensities for the first nine lines with Miller indices (00l) were measured from a film taken on a Guinier–Simon camera. The sample examined had a nominal composition of $Li_{0.2}NbSe_2$. Structure factors were calculated by using eq 1 (where the terms I_o, $F(00l)$, θ, θ_m, A, and p are respectively the measured intensity, the structure factor, the Bragg angle, the angle the X-ray beam makes with the monochromator, the absorption correction, and the multiplicity ($p = 2$ for all 00l lines)) and were fit to values calculated by eq 2. We assumed a two-layer repeat and space group $P\bar{3}$. Only (00l) lines were used to eliminate errors caused by preferential packing of the sample in the capillary. The function fit was

$$I_o \propto |F(00l)|^2 \frac{1 + \cos^2(2\theta_m)\cos^2(2\theta)}{(1 + \cos^2(2\theta_m))\sin^2\theta\cos\theta} Ap \qquad (1)$$

$$|F(00l)| = 2|f_{Nb}(\theta)\cos(2\pi l z_3) + f_{Se}(\theta)(\cos(2\pi l z_1) + \cos(2\pi l z_2))| \qquad (2)$$

where z_1, z_2, and z_3 are the positions of Se_1, Se_2, and Nb within the unit cell. The limited size of our data set put a constraint on our ability to confidently fit both thermal factors and an absorption correction; therefore, we fit only the absorption factor. The atomic scattering factors, $f_n(\theta)$, are given by $f_n(\theta) = f_n^0(\theta)\exp[(-B\sin\theta^2)/\lambda^2]$. Values for atomic scattering factors were taken from ref 8, and the thermal parameters, B_{Nb} and B_{Se}, are estimated from room-temperature values reported for similar dichalcogenides[9,10] ($B_{Nb} = 2.0$, $B_{Se} = 1.5$). Values of the absorption correction for cylindrical samples as a function of μR were taken from ref 8. A value of 4.3 for μR gave the best fit, where μ is the absorption coefficient and R is the capillary radius. We obtain reasonable agreement for lines with $l > 2$, as listed in Table II. The 003 and 005 lines were not distinguishable from the background noise so they are taken to have zero intensity. The 001 line was obscured in both the Guinier and Debye–Scherrer patterns. Si was used as an internal standard for line position determination.

Table II. Structure Factors and d Spacings from Fit to $Li_{0.2}NbSe_2$

hkl	d_o	d_c	F_o	F_c	$F_o - F_c$
001		12.930		9.0	
002	6.460	6.465	71.1	71.5	−0.3
003		4.310	0.0	0.9	−0.9
004	3.234	3.233	47.6	45.0	2.5
005		2.586	0.0	1.2	−1.2
006	2.156	2.155	60.6	62.1	−1.5
007	1.849	1.847	44.7	42.2	2.5
008	1.618	1.616	113.7	113.6	0.1
009	1.438	1.437	34.6	37.6	−3.0

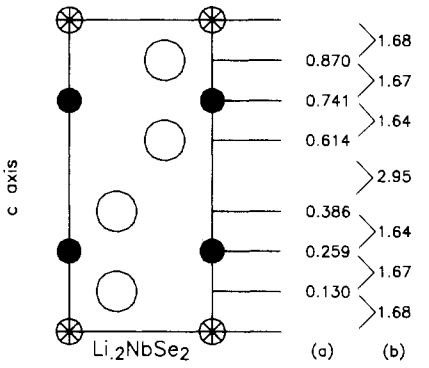

Figure 5. 110 projection of $Li_{0.2}NbSe_2$ showing (a) crystallographic positions (z) and (b) the distance between atomic planes in angstroms. ● and ○ represent Nb and Se, respectively; circled astrisks represent possible Li sites which are partially occupied.

Figure 5 summarizes the salient features. The atom positions z_1, z_2, and z_3 were found to be 0.130, 0.386, and 0.259 with an estimated error of ±0.001. These values compare with unintercalated $NbSe_2$ values of 0.116, 0.384, and 0.250.[11] The z values obtained were quite independent of the thermal factors and the absorption correction used with values of $z_1 = 0.129$, $z_2 = 0.386$, and $z_3 = 0.259$ obtained when both of these correction factors were set to zero. The asymmetric spacing of the layers in the unit cell suggests staging of the lithium intercalate. The two van der Waals gaps are significantly different, one gap being 2.948 Å (as compared to 2.910 Å for the unintercalated material) while the other gap is somewhat larger at 3.362 Å. Although the layers move within the unit cell, the layer thickness, as measured by the intralayer Se–Se distance, does not change significantly upon lithium intercalation (3.36 Å for unintercalated vs. 3.31 Å for intercalated). Within each layer there is a slight asymmetry in the Nb–Se bond lengths, the two Nb–Se distances being 1.668 and 1.642 Å.

We do not claim our proposed structure is unique solution, yet it gives a plausible account of the intensities. Similar results have been obtained for $Rb_{0.2}NbSe_2$[12] and $Ag_{0.19}TiS_2$.[9] In both of these intercalate systems the layer thickness was shown to remain constant upon intercalation and the TiS_2 system exhibited marked asymmetries in the Ti–S distances within each layer.

Since lithium is such a poor scatterer, it was not included in our fit. We suggest that the lithium is located in the larger van der Waals gap as indicated in Figure 5. Lithium, with an ionic radius of 0.9 Å, would fit too snugly into the approximately 0.75-Å octahedral sites in the narrower gap but could fit easily into the larger gap's 0.88-Å sites. The 0.45-Å expansion of the larger gap is nearly the same as the 0.5 Å/layer expansion for our $x = 1$ sample. With lithium in the larger gap, the slight polarization of the layers could be explained in terms of lithium–niobium

(7) Revolinsky, E.; Spiering, G. A.; Beernsten, D. J. *J. Phys. Chem. Solids* **1965**, *26*, 1029.
(8) "International Tables for X-ray Crystallography"; Kynoch Press: Birmingham, England, 1962; Vol. III. "International Tables for X-ray Crystallography"; Kynoch Press: Birmingham, England, 1974; Vol. IV.
(9) Mori, M.; Ohshima, K.; Moss, S. C.; Frindt, P. F.; Plischke, M.; Irwin, J. C. *Solid State Commun.* **1982**, *43*, 781.
(10) Alcock, N. W.; Kjekshus, A. *Acta Chem. Scand.* **1965**, *19*, 79.
(11) Brown, B. E.; Beernsten, D. J. *Acta Crystallogr.* **1965**, *18*, 31.
(12) Bourdillon, A. J.; Pettifer, R. F.; Marseglia, E. A. *Physica B+C (Amsterdam)* **1980**, *99B+C*, 64.

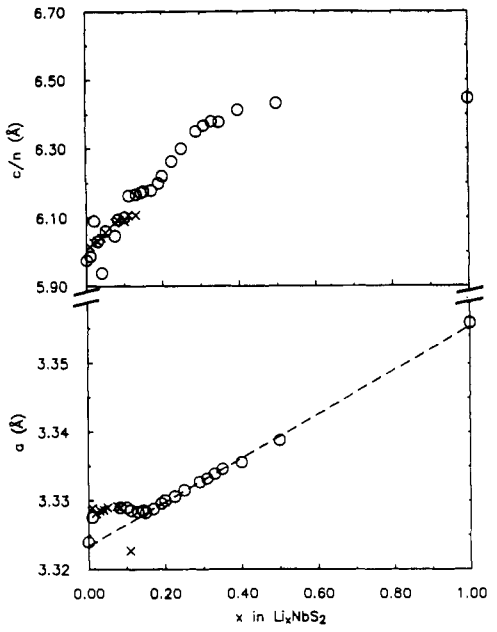

Figure 6. Lattice parameters vs. nominal composition in Li_xNbS_2. O and × represent data for 2H and 3R phases, respectively. The dashed line is a fit to data with $0.15 \leq x < 1$.

Table III. Li_xNbS_2 Lattice Parameters

x in Li_xNbS_2	a, Å[a,b]	c, Å[a,c]	polytype[d]
0.000	3.324	2× 5.98 (1)	2H
0.010	3.328 (9)	2× 5.986	2H
0.010	3.329	3× 6.015	3R*
0.020	3.49 (17)	2× 6.09 (7)	2H
0.020	3.328	3× 6.027	3R*
0.030	3.28 (4)	2× 6.03 (2)	2H
0.030	3.329	3× 6.031	3R*
0.040	3.15 (15)	2× 5.94 (8)	2H
0.040	3.329	3× 6.042	3R*
0.050	3.35 (2)	2× 6.061 (6)	2H
0.050	3.329	3× 6.057	3R*
0.075	3.27 (5)	2× 6.05 (2)	2H
0.075	3.329	3× 6.086	3R*
0.083	3.329	2× 6.094	2H
0.083	3.329	3× 6.092	3R*
0.100	3.329	2× 6.101	2H*
0.100	3.319 (10)	3× 6.090 (4)	3R
0.111	3.329	2× 6.163	2H*
0.111	3.323 (10)	3× 6.107 (9)	3R
0.130	3.328	2× 6.168	2H*
0.130	3.317 (6)	3× 6.108 (7)	3R
0.143	3.329	2× 6.173	2H
0.150	3.328	2× 6.177	2H
0.170	3.329	2× 6.179	2H
0.190	3.330	2× 6.199	2H
0.200	3.330	2× 6.220	2H
0.225	3.331	2× 6.264	2H
0.250	3.332	2× 6.299	2H
0.290	3.333	2× 6.349	2H
0.310	3.333	2× 6.367	2H
0.330	3.334	2× 6.380	2H
0.350	3.335	2× 6.377	2H
0.400	3.336	2× 6.413	2H
0.500	3.339	2× 6.432	2H
1.000	3.356	2× 6.446	2H

[a] Parentheses denote the estimated error for sample with larger errors. [b] ±0.001 Å. [c] ±0.002 Å. [d] An asterisk denotes the majority phase.

repulsion and attraction between lithium and the adjacent selenium atoms.

Li_xNbS_2. In the series Li_xNbS_2 the structural polytype varies with composition. For $x < 0.01$ the majority phase was found to be of the 2H-$NbSe_2$ polytype. For $0.01 \leq x < 0.10$ the 3R-MoS_2 polytype was prevalent and above $x = 0.10$ 2H was again the major polytype. Lattice parameters for this system are listed in Table III and plotted in Figure 6. We have plotted parameters for both polytypic phases together. Scatter in the data is due largely to the lack of precision in determining the lattice parameters for the minority polytype when two polytypes are present. The change of phase from 2H to 3R with the addition of small amounts of intercalate is reminicent of our previous work with nonstoichiometric NbS_2.[1] In that system the 3R polytype became prevalent when a small amount of excess niobium was intercalated between the layers. The use of large sulfur overpressures in the present investigation was designed to eliminate the possibility of excess niobium.

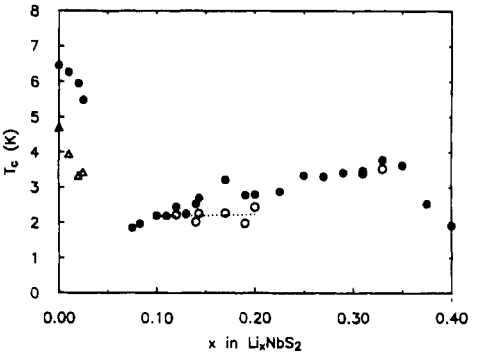

Figure 7. T_c vs. nominal composition for Li_xNbS_2. Δ and O represent the lower T_c's when multiple signals exist.

Table IV. Li_xNbS_2 Superconductivity Data

x in Li_xNbS_2	T_c, K	ΔT_c, K	x in Li_xNbS_2	T_c, K	ΔT_c, K
0.00	6.46	0.41	0.143	2.26	0.41
0.00	4.67	1.49	0.17	3.22	0.77
0.01	6.27	0.73	0.17	2.28	0.96
0.01	3.91	1.13	0.19	2.78	0.35
0.02	5.95	1.54	0.19	1.99	0.84
0.02	3.29	1.10	0.20	2.80	0.32
0.025	5.48	1.71	0.20	2.45	0.51
0.025	3.39	0.89	0.225	2.89	0.35
0.075	1.85	0.19	0.25	3.34	0.19
0.083	1.97	0.33	0.27	3.31	0.17
0.10	2.20	0.44	0.29	3.42	0.09
0.11	2.19	0.48	0.31	3.47	0.03
0.12	2.46	0.18	0.31	3.41	0.08
0.12	2.23	0.49	0.33	3.78	0.45
0.13	2.25	0.57	0.33	3.53	0.13
0.14	2.53	0.37	0.35	3.62	0.16
0.14	2.02	0.36	0.375	2.54	0.12
0.143	2.70	0.36	0.40	1.92	0.19

As lithium content increases, the a parameter at first undergoes a sharp rise, levels out, and then increases linearly for $x > 0.15$. The linear portion is similar to that for Li_xNbSe_2 but with slightly different slope. The data for $0.15 < x < 0.35$ extrapolates to an a parameter of 3.353 Å at $x = 1$. This value is in agreement with our low-temperature n-butyllithium result of 3.356 Å for $x = 1$. The 3R phase only appears at low x where the a parameter is flat, yet the a parameters for the 3R and 2H phases behave similarly with no discontinuous jumps. The c parameter of Li_xNbS_2 first increases rapidly and then changes very little for $x > 0.4$, similar to the Li_xNbSe_2 results. The value of c for $x = 1$ is 12.892 Å. Unlike Li_xNbSe_2 there appears to be a leveling off of c for $0.1 < x < 0.2$. The 3R polytype levels off to a slightly lower value than the 2H. Significantly, the four samples on the middle of this c plateau exhibit forbidden X-ray lines. As seen previously in $Li_{0.20}NbSe_2$, the extra lines suggest staging of the lithium in these materials.

The T_c behavior for Li_xNbS_2 is not at all similar to that for the Li_xNbSe_2 series (Table IV and Figure 7). The T_c at first drops precipitously from 6.46 K at $x = 0$ to below our detection limit at $x = 0.03$. The T_c then rebounds to 3.78 K at $x = 0.33$ only to drop again by $x = 0.40$.

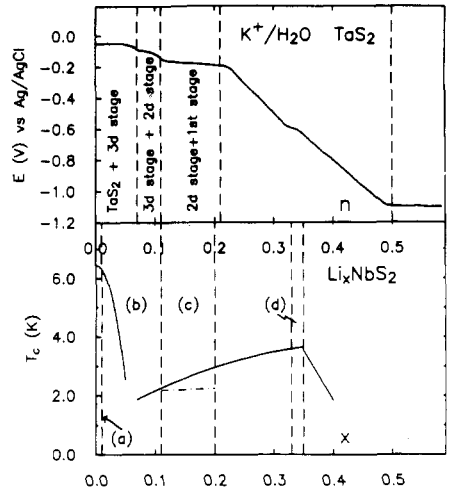

Figure 8. T_c vs. lithium content in Li_xNbS_2 as compared with Schollhorn's potential/charge-transfer curve (n = faraday/mol) for K^+/H_2O in TaS_2. Regions of 2H-NbS_2 (a), 3R-NbS_2 (b), mixed first and second stage (c), and possible intralayer Li ordering (d) are proposed.

Many of our samples are multiphased as evidenced by multiple superconducting transitions. The lower T_c's in the samples with $x < 0.03$ appeared only after a second grinding of the samples and, as these signals were rather weak, we attribute the second T_c to some unidentifiable minority phase. The samples in the range $0.12 < x < 0.20$ which exhibit two T_c's occur in the range where our X-ray evidence suggests ordering and/or staging. From Figure 7 it is evident that the lower T_c's in this range are almost constant with increasing x. The X-ray and T_c evidence taken together suggests a disproportionation of samples in this region into a staged and/or ordered material with constant T_c and a less perfectly staged or unstaged material with somewhat higher T_c.

Staging in alkali-metal intercalated transition-metal dichalcogenides has been suggested, and demonstrated, by a number of workers.[2,13,14] Figure 8 shows the results of the electrochemical intercalation of TaS_2 with K^+ as reported by Schollhorn, compared to our results. Schollhorn's data show a kink at $x = 0.33$, and other investigators have demonstrated ordering for intercalates near this composition.[13,15] Our samples with compositions near $x = 0.33$ also exhibit multiple T_c's, possibly indicative of ordering at low temperature, yet they display no anomalies in their room-temperature lattice parameters.

One sample, $Li_{0.15}NbS_2$, was investigated by electron diffraction, and weak supperlattice spots were detected when the samples were cooled to 240 K. The superlattice spots were found to have lengths of $3^{1/2}a_0$ and $2a_0$ which was indicative of lithium ordering within each layer. $3^{1/2}a_0$ superlattices have been found for intercalates with compositions near $x = {}^1/_3$,[14] and $2a_0$ superlattices arise for compositions near $x = {}^1/_4$.[17] Samples exhibiting both superlattices have also been observed.[15] With the compositions of interest lying between $x = {}^1/_6$ and $x = {}^1/_8$, we conclude that at low temperature we have both staging, lithium in every other layer, and intralayer ordering, lithium occupying every third or fourth octahedral site within each layer. Similar results have been reported for Ag_xTiS_2.[18]

The general behavior of T_c as lithium content is increased remains something of a mystery. We would expect T_c to eventually fall off as it does in the series Li_xNbSe_2, but the diminution and subsequent resurgence of T_c are quite unusual and cannot be described in terms of the usual band models. There does, however, seem to be some correlation between the predominance of the 3R phase and the reduction of T_c.

Conclusion

The systems Li_xNbSe_2 and Li_xNbS_2 demonstrate the complexity of structural behavior possible when transition-metal dichalcogenides are intercalated with alkali metals. The picture that emerges is one of lithium ordering both within and between the layers. The effect of band filling and ordering on one physical property, T_c, shows the sensitivity of this property to slight compositional variation even within the same sample. Comparison of materials synthesized at elevated temperatures and those intercalated at room temperature shows remarkable agreement.

Acknowledgment. This work was in partial fulfillment of the Ph.D degree of C.S.M. We would like to thank Dr. Stuart McKennan at the University of Bristol for the electron diffraction work. This research was sponsored by the National Science Foundation under Grant No. DMR 80-24050 and was supported in part by the Air Force Office of Scientific Research and the Materials Science Center at Cornell University. P.P.E. also thanks the SERC (U.K.) and NATO (Grant 250.81) for support.

Registry No. $LiNbS_2$, 55964-37-9; Li_xNbS_2, 56321-19-8; $LiNbSe_2$, 55964-36-8; Li_xNbSe_2, 61673-65-2; NbS_2, 12136-97-9; $NbSe_2$, 12034-77-4; Li_2S, 12136-58-2; Li_2Se, 12136-60-6; Nb, 7440-03-1; S, 7704-34-9; Se, 7782-49-2; *n*-butyllithium, 109-72-8.

(13) Schollhorn, R. *Physica B+C (Amsterdam)* **1980**, *99B+C*, 89.
(14) Zanini, M.; Shaw, J. L.; Tennenhouse, G. J. *Solid State Ionics* **1981**, *5*, 371.
(15) Thompson, A. H. *Physica B+C (Amsterdam)* 1981, *105B+C*, 461.
(16) Kleinberg, R. L.; Silbernagel, B. G.; Thompson, A. H. *Solid State Commun.* **1982**, *41*, 401. McKinnon, W. R.; Dahn, J. R. *Solid State Commun.* **1983**, *48*, 43.
(17) De Ridder, R. *Physica B+C (Amsterdam)* **1980**, *99B+C*, 39.
(18) Plischke, M.; Bardhan, K. K.; Leonelli, R.; Irwin, J. C. *Can. J. Phys.* **1983**, *61*, 397.